Plasmid 111 (2020) 102532

Contents lists available at ScienceDirect

Plasmid

journal homepage: www.elsevier.com/locate/yplas

Antimicrobial resistance gene shuffling and a three-element mobilisation system in the monophasic *Salmonella* typhimurium strain ST1030

M. Oliva[1], C. Calia[1], M. Ferrara[2], P. D'Addabbo[1], M. Scrascia[a], G. Mulè[b], R. Monno[c], C. Pazzani[a,*]

[a] Department of Biology, University of Bari, via Orabona, 4, 70125 Bari, Italy
[b] Institute of Sciences of Food Production, National Research Council of Italy (ISPA-CNR), Via G. Amendola 122/O, 70126 Bari, Italy
[c] Department of Basic Medical Sciences Neurosciences and Sense Organs Medical Faculty, University of Bari Piazza G. Cesare Policlinico, 70124 Bari, Italy

ARTICLE INFO

Keywords:
Monophasic variant 1,4,[5],12:i:-
IS*26*
Tn*21*-derived
I1 conjugative
ColE1-like
Orphan mob-associated *oriT*

ABSTRACT

In this study we describe the genetic elements and the antimicrobial resistance units (RUs) harboured by the *Salmonella* Typhimurium monophasic variant 1,4,[5],12:i:- strain ST1030. Of the three identified RUs two were chromosomal, RU1 (IS*26*-bla_{TEM-1}-IS*26*-*strAB*-*sul2*- IS*26*) and RU2 (IS*26*-*tetR*(B)-*tetA*(B)-ΔIS*26*), and one, RU3 (a *sul3*-associated class 1 integron with cassette array *dfrA12*-*orfF*-*aadA2*-*cmlA1*-*aadA1*), was embedded in a Tn*21*-derived element harboured by the conjugative I1 plasmid pST1030-1A. IS*26* elements mediated the antimicrobial resistance gene (ARG) shuffling and this gave rise to pST1030-1A derivatives with different sets of ARGs. ST1030 also harboured two ColE1-like plasmids of which one, pST1030-2A, was mobilisable and the target of an intracellular translocation of the Tn*21*-derived element; the second (pST1030–3) was an orphan *mob*-associated *oriT* plasmid co-transferred with pST1030-1A and pST1030-2A. pST1030-2A and pST1030-3 also carried a *parA* gene and a type III restriction modification system, respectively. Overall analysis of our data reinforces the role played by IS*26*, Tn*21*-derived elements and non-conjugative plasmids in the spread of ARGs and supplies the first evidence, at least in *Salmonella*, for the identification of a natural isolate harbouring a three-element mobilisation system in the same cell.

1. Introduction

Genetic elements such as insertion sequences (IS), transposons (Tn) and plasmids play a key role in the spread of antimicrobial resistance genes (ARGs) (Partridge et al., 2018). Among the IS, IS*26* plays a leading role in the mobilisation and spread of ARGs. In Gram-negative bacteria, IS*26* has been detected in chromosomes, Tn, and plasmids and associated with different ARGs (Harmer and Hall, 2015; He et al., 2015; Mollet et al., 1985; Moran and Hall, 2017; Oliva et al., 2018). IS*26* can move by a replicative mechanism which, when causing deletions of adjacent sequences, generates the so-called translocatable unit (TU) (Harmer et al., 2014). Integration of TU can occur through either an untargeted replicative (random insertion) or a conservative (targeting other IS*26* elements) mechanism (Harmer and Hall, 2016). The latter is responsible for the formation of multimeric arrays of IS*26* flanking DNA sequences (Harmer and Hall, 2017). In addition, the gene shuffling mediated by IS*26* within and between genetic elements triggers the arrangement of different sets of ARGs that might be horizontally transferable.

Among the Tn, Tn*21* and its derivatives have an important role in HGT in that they are widespread and harbour a large range of ARGs (Liebert et al., 1999). In Tn*21* and its derivatives ARGs are generally embedded in class 1 integrons (the class more broadly distributed in Proteobacteria), which are genetic elements able to integrate and express gene cassettes (Cambray et al., 2010; Domingues et al., 2015; Hall and Collis, 1995; Stokes and Gillings, 2011). In Tn*21* derivatives an IS*26* is often found within class 1 integrons at the end of the 3′-conserved segment (3'-CS) (*sul1*, *qacEΔ1* and *orf5*) interrupting the *tniA* gene (Moran and Hall, 2018). The junction between IS*26* and the remainder of *tniA* is conserved in both class 1 integrons containing *sul1* and the 3'-CS, and in the rarer *sul3*-associated class 1 integrons where the 3'-CS was replaced by the *sul3*-segment (*tnp440*-*sul3*-*orf1*-IS*26*) (Antunes et al., 2007; Curiao et al., 2011; Moran et al., 2016). The linkage among Tn*21*-derivative elements, class 1 integrons and conjugative plasmids and its relevance in HGT of ARGs has been widely documented (Partridge et al., 2009; Stokes and Gillings, 2011; Zheng et al., 2020). In *Salmonella*, an important foodborne pathogen, these elements have frequently been detected in FI, FII, HI1 and I1 plasmids (Cain and Hall, 2012; Miriagou et al., 2006; Oliva et al., 2018).

Conjugative plasmids that possess both relaxase and type IV

* Corresponding author.
E-mail address: carlo.pazzani@uniba.it (C. Pazzani).

https://doi.org/10.1016/j.plasmid.2020.102532
Received 3 June 2020; Received in revised form 4 August 2020; Accepted 5 August 2020
Available online 25 August 2020
0147-619X/

Table 1
Horizontal gene transfer.

Strain	Resistance(s)[a]	Resistance genes	Genome localisation	Transconjugant/Transformant strain (plasmid)	Resistance genes transferred by conjugation	Frequency of conjugation (SD)[e]	Resistance genes transferred by transformation
ST1030	ApCmSmSuTcTp	*dfrA12-aadA2-cmlA1-aadA1-sul3 blaTEM-strAB-sul2; tetR*(B)-*tetA*(B)	pST1030-1A[b] Chromosome	BA2A (pST1030-1A)	*dfrA12-aadA2-cmlA1-aadA1-sul3*	3.1 (± 2.7) × 10^{-3}	
				BA2B (pST1030-1B[b])	*dfrA12-aadA2-cmlA1-aadA1-sul3; tetR*(B)-*tetA*(B)	4.4 (± 4.6) x 10^{-8}	
				BA2C (pST1030-1C[b])	*dfrA12-aadA2-cmlA1-aadA1-sul3; bla_{TEM}-strAB-sul2; tetR*(B)-*tetA*(B)	6.6 (± 1.3) x 10^{-8}	
				BA2D (pST1030-2B[c])			*dfrA12-aadA2-cmlA1-aadA1-sul3*
BA2A	CmSmSuTp	*dfrA12-aadA2-cmlA1-aadA1-sul3*	pST1030-1A	BA2E (pST1030-1A)	*dfrA12-aadA2-cmlA1-aadA1-sul3*	1.3 (± 0.2) x 10^{-2}	
BA2B	CmSmSuTcTp	*dfrA12-aadA2-cmlA1-aadA1-sul3; tetR*(B)-*tetA*(B)	pST1030-1B	BA2F (pST1030-1B)	*dfrA12-aadA2-cmlA1-aadA1-sul3; tetR*(B)-*tetA*(B)	4.0 (± 0.7) x 10^{-2}	
BA2C	ApCmSmSuTcTp	*dfrA12-aadA2-cmlA1-aadA1-sul3; bla_{TEM}-strAB-sul2; tetR*(B)-*tetA*(B)	pST1030-1C	BA2G (pST1030-1C)	*dfrA12-aadA2-cmlA1-aadA1-sul3; bla_{TEM}-strAB-sul2; tetR*(B)-*tetA*(B)	2.2 (± 1.0) x 10^{-2}	
BA2H	ApCmSmSuTp	*bla_{TEM}-strAB-sul2*; *dfrA12-aadA2-cmlA1-aadA1-sul3*	pST1007-1D[d] pST1030-2B	BA2I (pST1007-1D)	*bla_{TEM}-strAB-sul2*	4.0 (± 2.1) x 10^{-2}	
				BA2L (pST1007-1D) (pST1030-2B)	*bla_{TEM}-strAB-sul2 dfrA12-aadA2-cmlA1-aadA1-sul3*	2.0 (± 1.3) x 10^{-3}	
BA2D	CmSmSuTp	*dfrA12-aadA2-cmlA1-aadA1-sul3*	pST1030-2B	none	none	none	

[a] Ampicillin (Ap); Chloramphenicol (Cm); Streptomycin (Sm); Sulfamethoxazole (Su); Tetracycline (Tc); Trimethoprim (Tp).
[b] I1 plasmid.
[c] ColE1-like plasmid.
[d] FII plasmid.
[e] Values represent the mean frequency (SD stands for Standard Deviation).

secretion systems (T4SS) represent only 28% of the plasmids identified in Proteobacteria (Smillie et al., 2010). In addition to these plasmids, those classified as mobilisable can also contribute to the HGT of ARGs or, not least, as a reservoir of ARGs. Subclassification of non-conjugative plasmids has recently been revised and the identification of specific genetic features that allow their mobilisation has contributed to further extending the potential role played by these genetic elements in the HGT (Ramsay and Firth, 2017). In this study we describe: i) the plasmid content (I1 and ColE1-like) harboured by the multidrug-resistant *S*. Typhimurium monophasic variant (STMV) 1,4,[5],12:i:- strain ST1030; ii) the ARG shuffling and their HGT; iii) the mobilisation of the two detected pST1030-2A and pST1030-3 ColE1-like plasmids (of which pST1030–3 was an orphan *mob*-associated *oriT*) (Ramsay and Firth, 2017), mediated by the conjugative pST1030-1A I1 plasmid.

2. Materials and methods

2.1. Bacterial isolates and antimicrobial susceptibility testing

The STMV ST1030 is a clinical strain isolated in Southern Italy in 2008 (De Vito et al., 2015). ST1030 was assigned to the monophasic variant 1,4,[5],12:i:- on the basis of the absence of the *fljB* gene tested by PCR (Echeita et al., 2001). Antimicrobial susceptibility tests were performed as reported previously (Oliva et al., 2017). The antimicrobials were: ampicillin (Ap), chloramphenicol (Cm), streptomycin (Sm), sulphamethoxazole (Su), tetracycline (Tc) and trimethoprim (Tp).

2.2. Bacterial conjugation, gene detection, plasmid typing and kinetic growth

Conjugation experiments were performed at 37 °C as described previously (Oliva et al., 2018). Antimicrobial concentrations used were: Ap 100 μg/mL, Cm 25 μg/mL, nalidixic acid (Nx) 50 μg/mL, rifampicin (Rf) 100 μg/mL, Sm 100 μg/mL, Su 600 μg/mL, Tc 20 μg/mL, Tp 30 μg/mL. Nalidixic acid-resistant CSH26 Nal or rifampicin-resistant DH5α Rf *Escherichia coli* strains were used as recipients. The frequency of transfer, mean number of transconjugants per donor, was determined in three or more independent experiments and the standard deviation (SD) calculated (Table 1). Plasmids were typed by the PCR Based Replicon Typing protocol (PBRT) using positive controls kindly supplied by A. Carattoli (Carattoli et al., 2005). Detection of ARGs, genetic elements and gene organization were performed by PCRs on ST1030, transconjugants and transformants. Primers used in this study were as reported previously (Camarda et al., 2013; Oliva et al., 2018) or newly designed (Table S1).

Kinetics of bacterial growth were performed as follows: o/n cultures of strains grown in Luria Bertani broth (LB) were diluted (1:10^4) in 100 mL of LB (T_0) in shake flasks and incubated at 37 °C. Samples were collected every hour (T_1 to T_8) and serial dilutions were plated on LB agar plates to assess the number of viable cells. The generation time (T_{gen}, time required to achieve a doubling of the population size) was estimated by determining the cell number (N) during the exponential phase (t) of active cell division and mathematically expressed using the following equation:

$$T_{gen} = t \log 2/(\log N_t - \log N_0)$$

2.3. DNA sequencing, assembly and annotation

Total genomic and plasmid DNA were extracted was extracted by the cetyl trimethylammonium bromide method (Murray and Thompson, 1980). About 1 μg of DNA was sheared with a Covaris M220 Focused-ultrasonicator (Covaris, Inc., MA, USA) with a target size of 400 bp and used for library preparation with the Ion Xpress Plus gDNA Fragment Library kit (Life Technologies, USA), following the manufacturer's instructions. Size selection of libraries (~400 bp) were performed by agarose gel electrophoresis using 2% *E*-Gel SizeSelect Agarose Gels (Life Technologies, USA). After purification, library concentrations were quantified using the Qubit dsDNA HS Assay Kit (Life Technologies, USA). Template-positive Ion Sphere Particles were prepared for 400-base-read using the Ion OneTouch 2 System (Thermo Fisher Scientific, Carlsbad, CA, USA) with an Ion 520 & 530 Kit-OT2 (ThermoFisher Scientific, USA) and then sequenced on an Ion 530 Chip using an Ion S5 System (ThermoFisher Scientific, USA). Raw data were quality filtered and assembled by using SPAdes assembler version 3.10.1 (Bankevich et al., 2012).

Contigs were assembled by specific PCRs and analysis of restriction profiles generated by specific enzymes (Fig. 4, Fig. S1 and Table S2). The genetic organization of pST1030-1B and pST1030-1C was deduced by comparing their *ClaI*, *HindIII* and *XhoI* profiles with those of pST1030-1A, and by specific PCRs. DNA sequences of pST1030-1A, pST1030-1B, pST1030-1C, pST1030-2A, pST1030-2B, pST1030–3 and the chromosomal region spanning from STM2746 to *iroC* (where the RU1 and RU2 were located) were deposited in GenBank under accession numbers MT507877, MT507880, MT507879, MT507878, MT507883, MT507881 and MT507882, respectively. STM refers to chromosomal genes as reported in *S*. Typhimurium referring strain LT2. DNA sequences of pST1030-1A derivatives can be obtained by IS*26*-mediated ARG shuffling (for details see section *3.3.1*). DNA sequence of pST1030-2B was obtained by insertion of the Tn*21*-derived element (harboured by pST1030-1A) into pST1030-2A (for details see section *3.4*).

Annotation was automatically performed using PROKKA (Seemann, 2014) and edited on the basis of its comparison with the well-characterised plasmids R64 (AP005147), ColIb-P9 (AB021078), pST1007-1A (MH257753), ColE1 (NC_001371) and NTP16 (L05392) and the chromosomal region of ST1007 (MH257754). Gene nomenclature for pST1030-1A was as that reported for R64 (Sampei et al., 2010).

2.4. Bioinformatic analysis

Similarity searches were performed using the BLASTN algorithm of the NCBI Web BLAST (https://blast.ncbi.nlm.nih.gov/Blast.cgi) using the pST1030-1A, pST1030-2A and pST1030–3 sequences as query. Results were graphically depicted by SnapGene (http://www.snapgene.com/) and Adobe Illustrator (https://www.adobe.com/it/). Putative promoter sequences were predicted using the tool for promoter search in prokaryotic genomes (http://www.phisitr.org/) (Klucar et al., 2010). Secondary structures of single stranded RNA or DNA sequences were predicted through the ViennaRNA Web Services (http://tbi.univie.ac.at/RNA/) (Gruber et al., 2008; Lorenz et al., 2011). Multiple sequence alignments were performed through the tool "MUSCLE" (https://www.ebi.ac.uk/Tools/msa/muscle/) (Madeira et al., 2019).

3. Results

3.1. Genome sequence of ST1030 and context of resistance genes

ST1030 is an STMV isolate which is part of a collection of 113 clinical MDR *S*. Typhimurium strains isolated in Italy between 2006 and 2012 (De Vito et al., 2015). Analysis of the ST1030 genome sequence revealed that in addition to the chromosome, three extrachromosomal replicons were detected: a conjugative I1 (pST1030-1A) and two mobilisable ColE1-like (pST1030-2A and pST1030–3) plasmids.

The ApCmSmSuTcTp resistance pattern, exhibited by ST1030, was encoded respectively by bla_{TEM-1}, *cmlA1*, (*aadA1*, *aadA2*, *strAB*), (*sul2*, *sul3*), *tetR*(B)-*tetA*(B) and *dfrA12* genes organised into three resistance units (RUs) (Fig. 1).

RU1 and RU2 were localised in the chromosome and flanked by IS*26* (Fig. 1A). RU1 (IS26_1-bla_{TEM-1}-IS26_2-*strAB*-*sul2*- IS26_3), a Tn*6029E* (a variant of Tn*6029*) (Reid et al., 2015), was inserted into STM2753; RU2 (IS26_4-*tetR*(B)-*tetA*(B)-IS1- ΔIS26_5), which contains regions derived

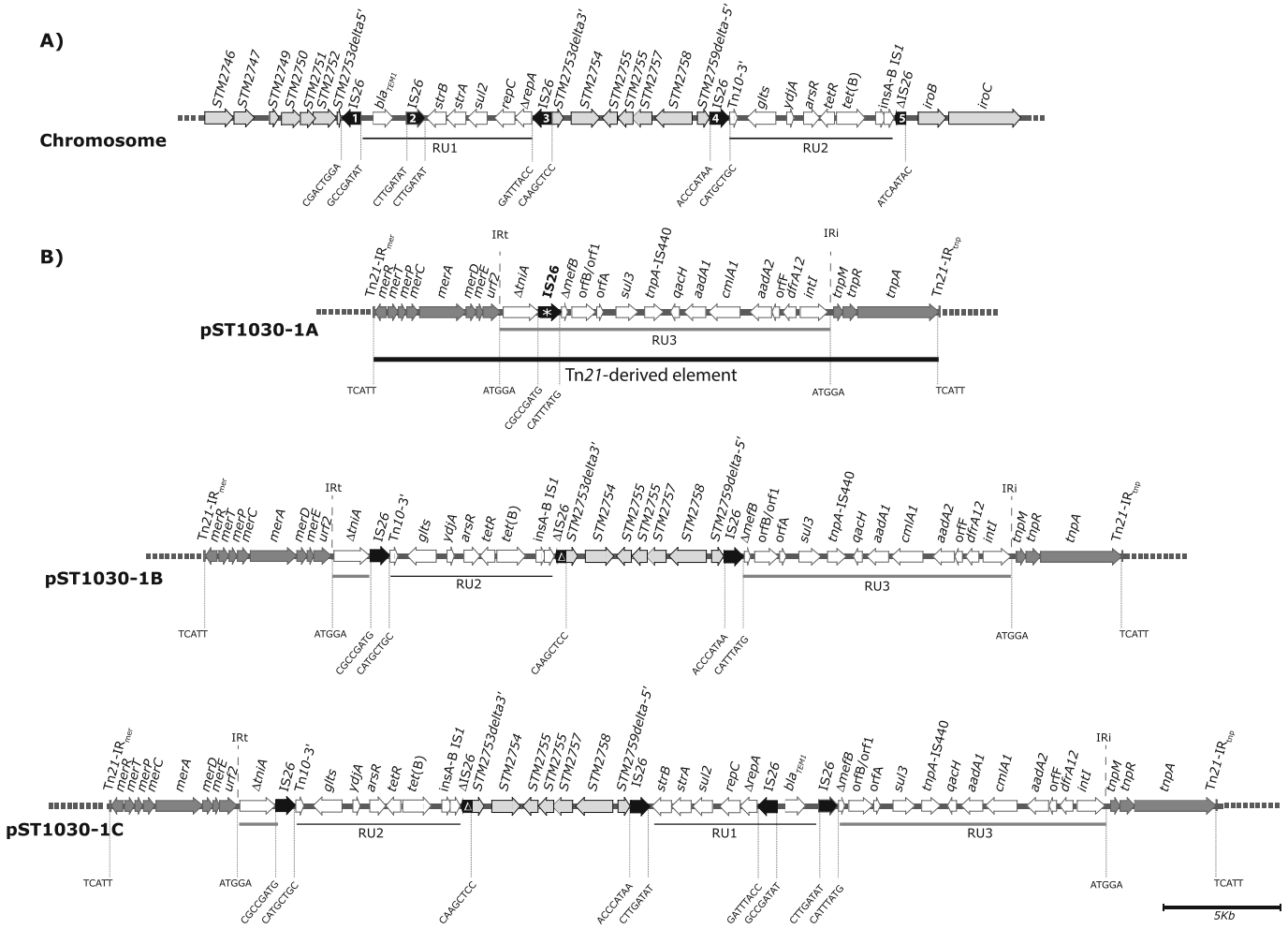

Fig. 1. Genomic localisation of resistance units (RUs) in ST1030.
Genes and open reading frames are shown as arrows pointing in the direction of transcription. RUs and chromosomal genes are indicated with white and light grey arrows, respectively. Dark grey arrows delimit the extent of the Tn*21*-derived elements flanking the RUs. Strait thin black lines indicate RU1 and RU2. The thick grey and black lines indicate the *sul3*-associated class 1 integron (RU3) and the extent of the Tn*21*-derived element, respectively. The sequence and position of both the 8-bp flanking the IS*26* and the target site duplications are indicated in capital letters. A) Chromosomal region harbouring RU1 and RU2 (GeneBank accession number MT507882). IS*26* are numbered and indicated with black arrows. The IS*26* number 5 is a ΔIS*26*, it lacks 129 bp that include both 77 bp 3′-*tnp26* and IRR. B) Linear representation of the distinguishing features between pST1030-1A and its derivatives. The IS*26* present in pST1030-1A is marked with an asterisk (*). The ΔIS*26*, is shown with the symbol delta (Δ).

from Tn*10* (Foster et al., 1981), was inserted into STM2759. The two IS*26* flanking RU1 were directly oriented; while those flanking RU2 were inversely oriented. The chromosomal region between $IS26_3$ and $IS26_4$ could be found in both possible orientations: 3'STM2753–5'STM2759 or 5'STM2759–3'STM2753 (this was demonstrated by PCR and enzyme restrictions of amplicons, Table S2). Similarly to what has been reported for the *S*. Typhimurium strain ST1007 (Oliva et al., 2018), RU1 and RU2 of ST1030 were found integrated in the same position in STM2753 (with the same 322 bp deletion of this gene) and ST2759, respectively. The $\Delta IS26_5$ lacked 129 bp that included the 77 bp 3′-*tnp26* and the IRR; this was demonstrated by PCR and sequencing of the DNA amplicon (Fig. S1 and Table S2). The *iroB* gene was found next to $\Delta IS26_5$. The chromosomal region from 3'STM2759 to *fljA-fljB-hin* was missing and this accounted for the monophasic variant of ST1030.

RU3 included a *sul3*-associated class 1 integron with the cassette array *dfrA12-orfF-aadA2-cmlA1-aadA1*, that was embedded in a Tn*21*-derived element harboured by pST1030-1A (Fig. 1B). The *sul3*-associated class 1 integron was flanked by imperfect inverted repeats of 25-bp (IRi and IRt), bounded by a 5-bp direct duplication of the target site and inserted in the same position as In2 in Tn*21* (Liebert et al., 1999). RU3 also contains an IS*26* element inserted between the truncated *mefB* and *tniA* genes.

3.2. ST1030's I1 plasmids

pST1030-1A consisted of 112,087 bp and comprised of a 91,242 bp backbone (50% GC), the 20,840 bp Tn*21*-derived element and a 5 bp target site duplication (TSD) generated by insertion of a Tn*21*-derived element into the backbone (Fig. 2). The pST1030-1A assembly was confirmed by comparing its restriction profiles obtained with *Cla*I, with the patterns generated by in silico restriction of its DNA sequence (Table S3). The pST1030-1A genome is organised into five major functional regions: replication, drug resistance, stability, leading and transfer. The complete genome sequences of R64 (AP005147) (Sampei et al., 2010) and ColIb-P9 (AB021078), the prototypes of the IncI1 group plasmids, were used for comparison.

The replication region was very similar to R64 and ColIb-P9 with nucleotide identities of 100% for *inc* and *repY*; and 94% for *repZ*. The drug resistance region included the *sul3*-associated class 1 integron embedded in the Tn*21*-derived element. The *sul3*-associated class 1 integron was similar to that identified in pCERC3 (a ColV virulence-

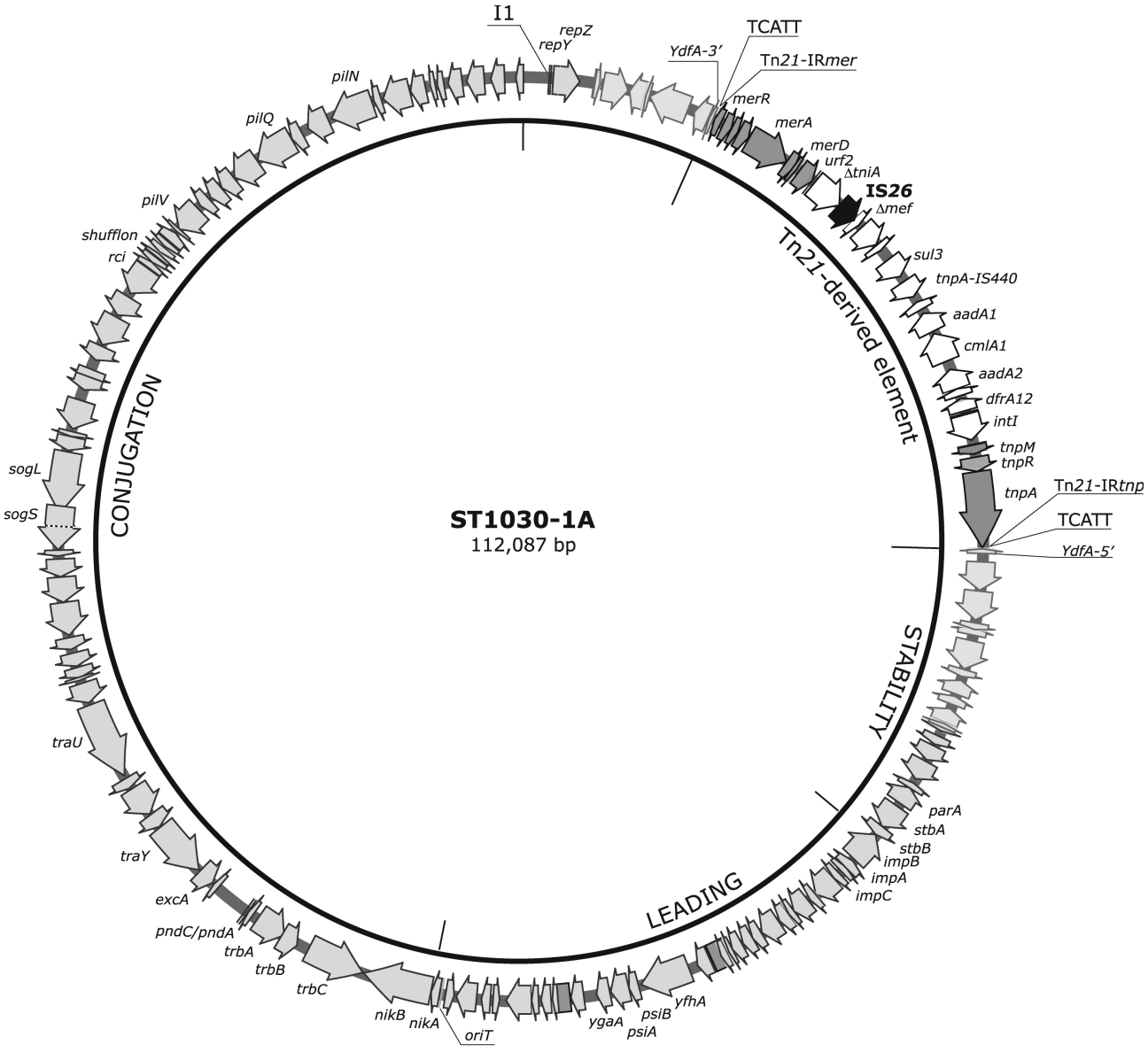

Fig. 2. Circular map of pST1030-1A.
pST1030-1A is drawn to scale (GeneBank accession number MT507877). Genes and open reading frames are shown as arrows pointing in the direction of transcription. Only some genes or operons are labelled. Genes associated with replicative, stability, leading and conjugative regions are in light grey. Dark grey arrows flank the *sul3*-associated class1 integron (white arrows) and delimit the extend of the Tn*21*-derived element. The back arrow highlights the IS*26*. The target site duplication sequence is shown in capital letters.

multidrug resistance plasmid isolated from a commensal *E. coli* strain) (Moran et al., 2016) and identical to that detected in pST1007-1A (a mosaic conjugative FII plasmid isolated from the clinical MDR *S*. Typhimurium strain ST1007) (Oliva et al., 2018). As in the case of pST1007-1A, the Tn*21*-derived element of pST1030-1A was inserted into *ydfA* (generating a 5-bp direct duplication) and contained a single copy of IS*26* while the Tn*21*-derived element harboured by pST1007-1A contained a second IS*26* element inserted into the *tnpR* of the Tn*21*-module. The stability region contained few homologies with the stability regions of R64 or pColIb-P9. These homologies were mainly restricted to *orfs* next to pST1030-1A *oriV*. However, when the stability region of pST1030-1A was searched as a query in GenBank sequences, it proved to be nearly identical (≥90%, with query cover of 100%) to other IncI1 plasmids detected in *S*. Typhimurium, STMV and *E. coli* strains (accession numbers JF274993, JQ901381, CP030921, CP039604, LT95504). The stability region of pST1030-1A ended with the partitioning system *stbA-stbB*. The leading region was similar (nucleotide identity ranging from 95 to 99%) to those of R64 and ColIb-P9. A notable difference was that shared for *ygaA*: homologous only with R64; ColIb-P9 contained *ydcA* rather than *ygaA*.

pST1030-1A *oriT* was nearly identical (81/83 nt) to the minimal sequence of R64 *oriT* (Furuya and Komano, 1997). The two mismatches detected in pST1030 *oriT* were complementary to each other in the formation of the stem-loop of the 17 bp inverted repeat involved in the termination of DNA transfer (Fig. S2). The gene organization of the transfer region was similar to R64 and ColIb-P9 with a nucleotide identity ranging from 97 to 99%. Lower identities were detected for *excA* (75% restricted to the 501 nt 3′ end) and *traY* (86% over the entire gene with 72% identity restricted to the 1066 nt 3′ end). The *traD* of R64 was not detectable and, in its place, an *orf* identical to *trcD* of ColIb-P9 was found. The shufflon region of pST1030-1A contained the four segments A, B, C and D found in R64 (Brouwer et al., 2015).

Results by searching and aligning GenBank sequences, using the pST1030-1A sequence as query detected no identical plasmids. The

most similar plasmids (coverage > 95% and identity > 98%) were: pSal8934a (JF274993), p12–6919.1 (CP039604), II (LT795504), Plm (JQ901381), pS68 (KU130396), A (CP010130), pUY_STM96 (MN241905), pUR-EC07 (MH674341). Plasmids were isolated from *E. coli*, *S.* Typhimurium or STMV. Interestingly, these plasmids harboured a nearly identical fragment previously described in pST1007-1A and name fragment C. However, none of the detected I1 plasmids (apart from the plasmid II), contained a Tn*21*-derived element inserted within the fragment C. In plasmid II the Tn*21*-derived element was not inserted into *ydfA* but into *ydfB*. The Tn*21*-derived element of plasmid II was nearly identical to the Tn*21*-derived element harboured by pST1030-1A. It differed only in 3 nucleotide mismatches of which one was localised in the *tnp26* (replacement of the leucine in position 110 of Tnp26 by an isoleucine), the other two were found in the genes *aadA1* and *tnpA* of the Tn*21*, respectively. These last mismatches were in the third base and did not affect the amino-acid sequences.

pST1030-1B and pST1030-1C were from insertion of IS*26*-mediated TUs originated from the chromosomal RUs (Fig. 1B): TU1 derived through recombination of the two directly orientated IS*26* (IS26_1 and IS26_3) that flanked RU1; TU2 through recombination of the two directly orientated IS*26* (IS26_3 and ΔIS26_5) that encompassed RU2 and the chromosomal gene cluster 3'STM2753–5'STM2759 (Fig. 1A). Insertion of TU2 into the IS*26* present in the Tn*21*-derived element of pST1030-1A accounted for the formation of pST1030-1B. For pST1030-1C two possible molecular processes have been hypothesised: i) insertion of TU1 into pST1030-1B; ii) insertion of the cointegrated TU1–2 (generated by recombination between TU1 and TU2) into pST1030-1A. It is noteworthy that detection of transconjugants harbouring either pST1030-1B or pST1030-1C was rare (mean frequency of 4.4×10^{-8} and 6.6×10^{-9} TC/D, respectively) (see paragraph 3.4). Tnp26-catalysed exchange between IS*26* elements occurs via crossover between either the two left or the two right ends of the IS elements (Harmer and Hall, 2017). In the case of TU2 recombination between ΔIS26_5 and IS26_3 could only happen between the two left ends, leaving an integral IS*26* on the chromosome and the ΔIS26_5 in the TUs (this was demonstrated by PCR and enzyme restrictions of amplicons, Fig. S1 and Table S2).

3.3. ST1030's ColE1-like plasmids

The pST1030-2A and pST1030–3 ColE1-like plasmids consisted of 5055 and 6760 bp, respectively (Fig. 3). The complete sequences of the widely studied ColE1 (Chan et al., 1985) and NTP16 (Cannon and Strike, 1992) plasmids were used for comparison.

pST1030-2A comprises a backbone of ~3,3 kb and a variable region of ~1,7 kb. The backbone was composed of the regions: mobilisation (*mbeA*, *mbeB*, *mbeC*, *mbeD*, *mbeE* and *oriT*), replication (*oriV* and *rop*) and recombination. *Rop* of pST1030-2A was 98% identical to *rop* of ColE1. ST1030-2A *oriT* was 98.7% identical in 79 bp overlap with the 83 bp minimal length of ColE1 *oriT* (Varsaki et al., 2009). The recombination region was comparable to the *cer* site of ColE1, sharing an identical *Arg-box* sequence and similar XerC (3 nucleotide mismatches) and XerD (3 nucleotide mismatches) binding sites (Fig. S3). The variable region contains the gene *parA*. The predicted ParA protein is a member of the P loop GTPase superfamily, SIMIBI class (Leipe et al., 2002). In particular, ParA of pST1030-2A is ascribable to the distinct subgroup called "orphan ParAs" (Lutkenhaus, 2012). Orphan ParAs are not associated with the usual partner ParB and are characterised by the "deviant Walker A motif – XKGGXXK[T/S]" that contains two conserved lysines of which the second is common to all walker motifs and required for binding and hydrolysis of ATP; the amino terminal lysine, called "lysine signature", is unique to this subgroup (Lutkenhaus and Sundaramoorthy, 2003).

pST1030-2B, as deduced by analysis of both its DNA sequence and restriction profiles, derived from insertion of the Tn*21*-derived element into *mbeC* of pST1030-2A (Fig. 3). The insertion resulted in a 5-nt (5'-TACTT-3') duplication of the target site and *mbeC* was split into a 5'-segment of 69-bp and a 3'-segment of 284-bp (referred to as Δ*mbeC*). Insertion of the Tn*21*-derived element also generated the sequence 5'-CCTACT-3' (overlapping the Tn*21*-IR_{mer} and the 5 bp target site) that is consistent with a putative −10 sequence promoter. The 5'-TTTCCG-3' sequence (putative −35 sequence promoter) found 15 bp upstream of the −10 sequence, generated a potential new promoter (Shimada et al., 2014). Putative transcription and translation of Δ*mbeC* would have produced a ΔMbeC of 81aa that retained the conserved amino acid domain (aa 26 to 68) of the superfamily bacterial mobilisation protein MobC and the NLN motif possibly involved in the interaction with any of the proteins implicated in conjugal mobilisation (Marchler-Bauer et al., 2017; Varsaki et al., 2009). MbeC has been hypothesised to interact through its C-terminal region with the N-terminal region of the MbeA relaxase, guiding MbeA to the *nic* site of *oriT*. MbeC also retains an additional functional motif (ribbon-helix-helix) localised in its N-terminal region that would recognise a DNA sequence of *oriT* next to the *nic* site (Varsaki et al., 2012). Therefore, it has been suggested MbeC plays a role in the efficient mobilisation of ColE1.

pST1030–3 comprises a backbone of ~1,9 kb and a variable region of ~4,8 kb (Fig. 3). The backbone was composed of the regions: replication (*oriV* and *rop*), transfer (*oriT*) and recombination. There was 67.4% identity (in 184 bp) between *rop*(s) of pST1030–3 and pST1030-2A with an amino acid sequence homology of 78% over the entire proteins. ST1030–3 *oriT* was 93.1% identical in 72 bp overlap with the 83 bp minimal length of ColE1 *oriT* (Varsaki et al., 2009). Next to *rop*, pST1030–3 contains a region of 82 bp similar (85.4% identity) to the *oriT* sequences of both R64 and pST1030-1A. This region included the sequences recognised by R64 NikA. The recombination region was comparable to the *nmr* site of NTP16, sharing an identical *Arg-box* sequence and a very similar XerC (1 nucleotide mismatch) and XerD (1 nucleotide mismatch) binding sites (Fig. S3). The variable region contains two ORFs of 1866 and 2637 bp encoding for putative type III N6-adenine DNA methyltransferase (M) and Type III restriction (R), respectively (Roberts et al., 2015).

Replication of ColE1 plasmids is mediated by an RNA pre-primer (RNA II) that forms a stable hybrid with the DNA in the origin region. Replication control is modulated by the antisense-RNA (RNA I) which is transcribed from the complementary strand in the 5′ pre-primer region (Brantl, 2014; Camps, 2010). The RNAII of pST1030-2A and pST1030–3 share identity with the RNAII of ColE1 and NTP16 only in the 3′ terminal 360 bp. The respective RNAI sequences of these plasmids were, as a whole, different to one other (Fig. S4). Analysis of the predicted secondary structures of RNA I and RNA II highlighted similar sequence domains (stems and loops) between pST1030–3 and NTP16; no conserved stems or loops were detected between pST1030-2A and ColE1 or NTP16. The −35 and − 10 sequences of RNAI and RNAII of pST1030-1A, pST1030–3 and ColE1were conserved; the promoter sequence of NTP16 for RNAII was different. The incompatibility determinants of ColE1-like plasmids are specific regions of RNA I/RNAII as demonstrated by point mutations generated in the region of RNA I/RNA II overlap or by the different RNAI sequences that allowed ColE1 to coexist with RSF1030 a plasmid closely related to NTP16 (Cannon and Strike, 1992; Tomizawa and Itoh, 1981). The presence of pST1030-2A and pST1030–3 in the *Salmonella* strain ST1030 could then be explained by the different RNA I sequences of these plasmids.

Searching for pST1030-2A sequence as query only produced a single record (plasmid pSUH-5, Acc. N° CP041342) with a query cover of 100% (nucleotide identity ≥95%). pSUH-5 was detected in *E. coli* isolated from human blood in Sweden in 2008. We also performed a search using the *parA* sequence with a query cover of 100%. Apart from pSUH-5 where the nucleotide identity for *parA* was 99,6%, results showed only nine records (Acc. N° CP043517; KU302809; CP041060; CP036334; CP033951; CP035127; CP036324: CP023572; CP027113) with nucleotide identity for *parA* ranging from 85,8 to 94,1%. Records were from plasmids isolated from either *E. coli*, *Klebsiella pneumoniae* or

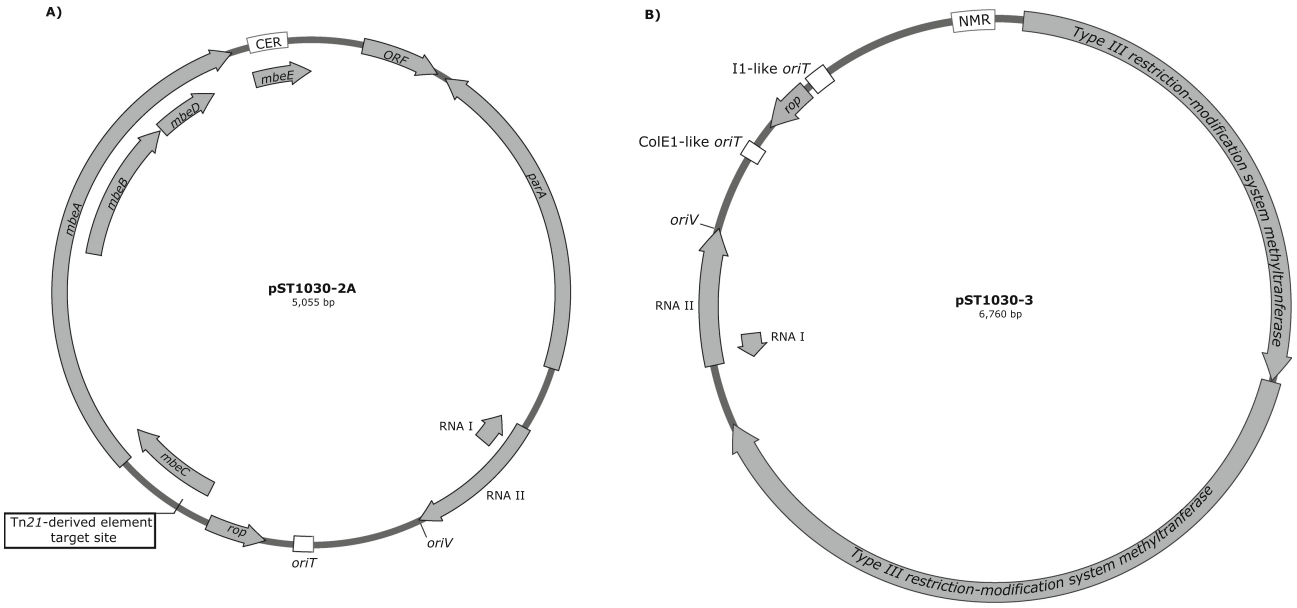

Fig. 3. Circular map of pST1030-2A and pST1030–3.
Genes and open reading frames are shown as arrows pointing in the direction of transcription and, for each plasmid, genes are to scale. A) pST1030-2A (GeneBank accession number MT507878). The multimeric resolution (*cer*) and *oriT* sites are in white boxes. Vertical bars indicate the origin of replication (*oriV*) and the site of insertion of the Tn*21*-derived element that originated pST1030-2B. B) pST1030–3 (GeneBank accession number MT507881). The multimeric resolution (*nmr*), and ColE1-like and I1-like *oriT* sites are in white boxes. The vertical bar indicates the origin of replication (*oriV*).

Enterobacter spp. All plasmids contained *oriV*-ColE1-like sequences; the plasmids isolated from *Enterobacter* spp. (Acc. N° CP043517; KU302809; CP041060; CP023572; CP027113) also shared a partial nucleotide identity (from 88 to 94%) with the ColE1 *oriT*. The pST1030–3 sequence was found to be nearly identical (99% identity, ≥99% query cover) to six plasmids detected in *S. enterica* subsp. *enterica* (Acc. N° CP039594; CP033225; MG948564; CP025235; CP025274; CP037878). The *Salmonella* strains were isolated between 2005 and 2013 from different sources and countries (Table S4).

3.4. Conjugation and transformation results

Results of conjugation experiments and PCR detection revealed the transfer of three distinct resistance patterns (Table 1): i) CmSmSuTp (RU3) was transferred (pST1030-1A) with a mean frequency of 3.1×10^{-3} transconjugants per donor (TC/D); ii) CmSmSuTcTp (RU3-RU2) was transferred (plasmid pST1030-1B) with a mean frequency of 4.4×10^{-8} TC/D; iii) ApCmSmSuTcTp (RU3-RU2-RU1) was transferred (plasmid pST1030-1C) with a mean frequency of 6.6×10^{-9} TC/D. The transconjugant strains BA2A, BA2B and BA2C carrying the plasmids pST1030-1A, pST1030-1B and pST1030-1C, respectively, were used as donors in conjugation experiments with *E. coli* DH5α Rf used as the recipient strain. pST1030-1B and pST1030-1C were transferred with a mean frequency similar to that established for pST1030-1A (Table 1).

It was also proved possible to acquire the resistance pattern RU3 via transformation (strain BA2D). However, in this case the resistance markers were localised in the ColE1-like plasmid pST1030-2B.

Plasmid DNA (pST1030-1A, pST1030-1B and pST1030-1C) was extracted as previously described and analysis of their restriction fragments revealed the presence of both a common pattern and additional fragments for pST1030-1B and pST1030-1C (Fig. 4A, Table S3). Overall, these data highlighted pST1030-1A as the main conjugative plasmid harboured by ST1030; while pST1030-1B and pST1030-1C were plasmids derived from pST1030-1A through acquisition of RU2 and RU2-RU1, respectively. By contrast, restriction patterns generated for pST1030-2B were of a different size and number to those of pST1030-1A (Fig. 4B, Table S3). The genetic organizations of pST1030-1B and pST1030-1C were deduced by comparing their *ClaI*, *HindIII* and *XhoI* profiles with those of pST1030-1A and by specific PCRs (Fig. S1 and Table S2).

Mobilisation of pST1030-2B was assessed through conjugation experiments. pST1030-2B was initially transferred into BA1D, a CSH26-Nal strain harbouring a conjugative FII plasmid (pST1007-1D) that encodes resistance to ApSmSu. The strains BA2G (harbouring both pST1007-1D and pST1030-2B) and BA2D (harbouring only pST1030-2B) were then used as donors in conjugation experiments with DH5α Rf. pST1030-2B was transferred only from matings with BA2G (mean frequency of 2.0×10^{-3} TC/D) (Table 1).

We also investigated the co-transferring of pST1030-2A and/or pST1030–3 with pST1030-1A. One hundred colonies selected on agar plates supplemented with both nalidixic acid and trimethoprim, and from the maximal dilutions where transconjugants could be identified, were analysed to detect the presence of pST1030-2A and/or pST1030–3. The presence of pST1030-2A and pST1030–3 was established by enzyme restriction of the plasmid content from each analysed transconjugant and by PCR detection with specific primers targeting pST1030-2A or pST1030–3 (Table S2). pST1030-2A was co-transferred in 92% of transconjugants; pST1030-2A and pST1030–3 were both co-transferred in 56% of transconjugants; in 8% of transconjugants pST1030-1A was found to be singularly transferred. pST1030–3 was never found co-transferred alone.

The average generation-time, estimated at 21 min for the transconjugants BA2A (harbouring only pST1030-1A), BA2M (harbouring the additional pST1030-2A) and BA2N (harbouring both pST1030-2A and pST1030–3) (Table S5) led us to deduce that the presence of ColE1-like plasmids in transconjugants harbouring pST1030-1A seems not to affect their fitness cost.

4. Discussions

S. Typhimurium is one of the most commonly isolated serovars from humans, retail meats of diverse origins and the environment. It has arguably the broadest host and pathogenicity range of all serovars of *S. enterica* subsp. *enterica* (Paul et al., 2016). Its broad host-range spectrum exposes this serovar to a wide potential inflow and outflow of

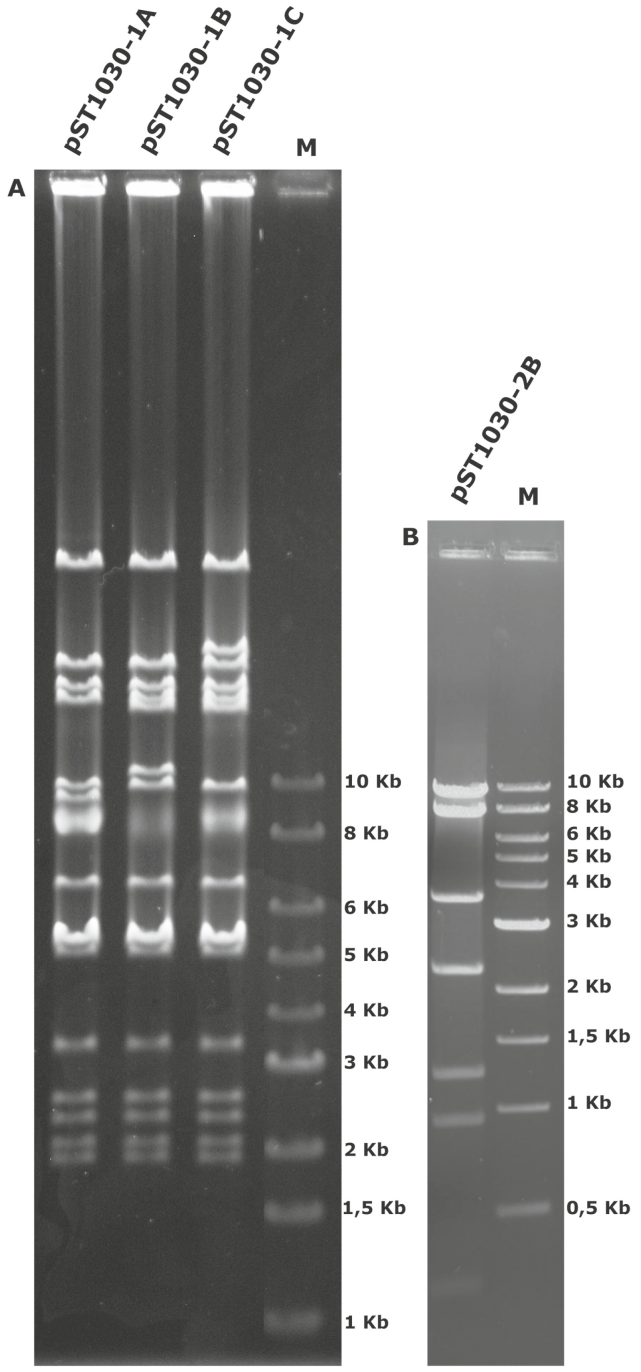

Fig. 4. Plasmid restriction patterns.
Plasmid names are reported above each line M: Quick Load 1 kb DNA Ladder (New England Biolabs). A) *ClaI* patterns. B) *EcoRI* pattern.

horizontally transmitted genetic elements such as plasmids. These last elements, as well as IS and Tn, are reported to play a key role in the spreading of ARGs and in the insurgence of MDR strains; the latter is now acknowledged as one of the emerging and most feared public health threats on a worldwide scale (Tanwar et al., 2014). In addition to conjugative plasmids, HGT of ARGs can also be mediated by non-conjugative mobilisable plasmids. The contribution of these plasmids is a matter of growing interest and research studies (Oliva et al., 2017; Ramsay and Firth, 2017; Rozwandowicz et al., 2018; Suhartono et al., 2018).

ST1030 is an MDR STMV strain that contains: i) two chromosomal RUs conferring resistance to ApSmSu (RU1) and Tc (RU2); ii) one conjugative I1 plasmid (pST1030-1A) harbouring a Tn*21*-derived element that confers resistance to CmSmSuTp (RU3); iii) two ColE1-like plasmids of which one mobilisable (pST1030-2A) and one identified as orphan *mob*-associated *oriT* (pST1030–3). This study has further highlighted the role played by IS*26* elements in the spread of ARGs. In ST1030, they mediated gene shuffling that generated a pool of conjugative I1 plasmids harbouring diverse sets of ARGs: *dfrA12-aadA2-cmlA1-aadA1-sul3* (pST1030-1A), *dfrA12-aadA2-cmlA1-aadA1-sul3-tetR*(B)-*tetA*(B) (pST1030-1B) and *dfrA12-aadA2-cmlA1-aadA1-sul3- tetR*(B)-*tetA*(B) bla_{TEM-1}-*sul2-strAB* (pST1030-1C). Transconjugants exhibiting resistance RU3-RU1 were not detected. It is possible that the absence of their detection might be due to a low frequency of formation of the cointegrate RU3-RU1. Moreover, the IS*26*-mediated gene shuffling also generated diverse Tn*21*-derived elements that might further spread the harboured ARGs within other bacterial genomes by intracellular translocation. pST1030-1A also shares an identical fragment C with a Tn*21*-derived element inserted into the same nucleotide position of *ydfA* with pST1007-1A (a mosaic FII conjugative plasmid isolated from the *S*. Typhimurium strain ST1007 collected in Apulia during the same, 2006–2008, three-year period) and, with the presence of a conserved TSD, this suggests a possible recent insertion of this element. The fragment C can only be detected, in silico, in I1 plasmids and we previously hypothesised that its presence in pST1007-1A reflected acquisition from I1 plasmids (Oliva et al., 2018). This hypothesis is further supported by the present study. A comparative analysis of the RUs between ST1030 and ST1007 showed the presence of two mismatches in RU1 (of which one determined the replacement of the glutamic acid at position 212 of StrA of ST1007 by an aspartic acid in ST1030); in RU2 the ΔIS*10*-left sequence of ST1030 (250 bp) was shorter than that in ST007 (340 bp) and also the RU2 of ST1030 lacked the sequence spanning from *merR* to the *ΔtniA* of the Tn*21*-derived element; the RU3 of both were identical.

The mobilisable pST1030-2A ColE1-like plasmid was efficiently co-transferred (92% of the analysed transconjugants) by pST1030-1A. The transfer efficiency of pST1030-2A mediated by pST1030-1A was higher than that reported for some ColE1-like plasmids such as NTP1 and NTP16 (frequency from 50 to 60%) co-transferred by R64 (Lambert et al., 1987), or by other plasmids harbouring *oriT*-like sequences of the co-resident conjugative plasmids (e.g pBuzz was co-transferred with an efficiency of 70% by the co-resident Inc. B/O p838B-R plasmid) (Moran and Hall, 2019). pST1030-2A was also the target of an intracellular translocation of the Tn*21*-derived element. This generated the pST1030-2B plasmid encoding for multidrug resistance. The Tn*21*-derived element became inserted into *mbeC* and a potential new promoter between the Tn*21*-IR_{mer} and the TSD was formed. This might allow transcription of Δ*mbeC* whose translated product (ΔMbeC) would retain the C-terminal function required to bind the N-terminal region of MbeA relaxase. However, ΔMbeC would not retain the N-terminal function possibly necessary to bind an *oriT* sequence next to the *nic* site. The horizontal transfer of pST1030-2B by the conjugative FII plasmid pST1007-1D raises open questions as to the possible role played by either the absence of MbeC or the presence of a ΔMbeC in the mobilisation of pST1030-2B. Moreover, pST1030-2A carries *parA* whose encoded protein is ascribable to “orphan ParAs” that are not associated with the usual partner ParB (Lutkenhaus, 2012). Actually, in addition to the three types of classical plasmid segregation systems there are data emerging that support the presence of other, as yet unknown, mechanisms that can ensure plasmid partitioning in each daughter cell during division (Guynet and de la Cruz, 2011). Whether the presence of *parA* in pST1030-2A is somehow related to a new segregation system remains to be explored.

The other identified ColE1-like plasmid (pST1030–3) was an orphan *mob*-associated *oriT* element. It lacked *mob* genes but harboured sequences of which one was nearly identical to ColE1 and pST1030-2A *oriT* and one similar to pST1030-1A and R64 *oriT*. pST1030–3 was co-transferred with pST1030-1A and pST1030-2A in 56% of

transconjugants harbouring these plasmids. In addition to mobilisable plasmids, those lacking Mob relaxase (conventionally described as non-mobilisable) may be mobilised *in trans* by conjugative elements if carrying a mimic of the conjugative element's *oriT* sequence (Ramsay and Firth, 2017). *oriT* mimicry plasmids have recently been described in *Staphylococcus* (Ramsay et al., 2016), *E. coli* (Moran and Hall, 2019), *Acinetobacter baumannii* (Blackwell and Hall, 2019) and *Citrobacter freundii* (Barry et al., 2019). Some *oriT* mimicry plasmids may also carry relaxosome accessory factors as reported for pCERC7 (a plasmid isolated in *E. coli*) that can be mobilised by R64 (Moran and Hall, 2017). Other non-mobilisable plasmids are defined as orphan *mob*-associated *oriT* (Ramsay and Firth, 2017). Mobilisation of these plasmids requires both a conjugative element and a *mob*-gene-carrying element. pST1030–3 is undoubtedly an orphan *mob*-associated *oriT* plasmid and, to the best of our knowledge, this is the first report (at least in *Salmonella*) of a natural isolate harbouring a three-element mobilisation system in the same cell. pST1030–3 also carries a Type III restriction modification (R-M) system. Type III R-M systems are present in a large number of sequenced bacterial genomes (Rao et al., 2014). The widespread nature of these systems indicates their importance, despite many aspects of their biological function remaining to be established. Whether the presence of a Type III R-M system in pST1030–3 confers a mutual benefit for both plasmid and host or merely a plasmid benefit remains to be explored.

In most STMV strains isolated worldwide from humans, animals, foods and environmental sources an IS*26* copy was detected next to *iroB* (Boland et al., 2018). This suggested a possible common ancestor for the globally observed STMV identified in recent years. It has thus been proposed that insertion and recombination of IS*26* elements has probably been the driving force behind the genetic variability of the STMV population (Boland et al., 2018). However, in ST1030 the IS*26* element next to *iroB* is interrupted by an IS*1* element. IS*1*-mediated intramolecular rearrangements have been documented (Turlan and Chandler, 1995) and the ST1030 chromosome harbours five IS*1* elements of which one has a perfect TSD, indicating the presence of a recent IS*1* integration. We cannot exclude the possibility that an IS*1*-mediated deletion between the IS*1* present in the Tn*21*-derived element and an IS*1* copy inserted into the IS*26*, originally next to *iroB*, triggered the loss of the chromosomal region from 3'STM2759 to *fljA-fljB-hin*.

The present study, in our view, reinforces the role played by different genetic elements in the spread of ARGs. It also supplies new data on features harboured by non-conjugative plasmids that increasingly emerge as a dynamic and complex group of the fascinating world of plasmids.

Supplementary data to this article can be found online at https://doi.org/10.1016/j.plasmid.2020.102532.

Acknowledgements

Very many thanks to thank Karen Laxton for writing assistance. Special thanks are also due to Dr. Francesca Fanelli (ISPA-CNR) and Dr. Cosma Liuzzi for preparing libraries and sequencing.

References

Antunes, P., et al., 2007. Dissemination of sul3-containing elements linked to class 1 integrons with an unusual 3′ conserved sequence region among Salmonella isolates. Antimicrob. Agents Chemother. 51, 1545–1548.
Bankevich, A., et al., 2012. SPAdes: a new genome assembly algorithm and its applications to single-cell sequencing. J. Comput. Biol. 19, 455–477.
Barry, K.E., et al., 2019. Don't overlook the little guy: an evaluation of the frequency of small plasmids co-conjugating with larger carbapenemase gene containing plasmids. Plasmid 103, 1–8.
Blackwell, G.A., Hall, R.M., 2019. Mobilisation of a small Acinetobacter plasmid carrying an oriT transfer origin by conjugative RepAci6 plasmids. Plasmid 103, 36–44.
Boland, C., et al., 2018. A liquid bead array for the identification and characterization of fljB-positive and fljB-negative monophasic variants of Salmonella typhimurium. Food Microbiol. 71, 17–24.
Brantl, S., 2014. Plasmid replication control by antisense RNAs. Microbiol. Spectr. 2 (PLAS-0001-2013).
Brouwer, M.S., et al., 2015. IncI shufflons: assembly issues in the next-generation sequencing era. Plasmid 80, 111–117.
Cain, A.K., Hall, R.M., 2012. Evolution of a multiple antibiotic resistance region in IncHI1 plasmids: reshaping resistance regions in situ. J. Antimicrob. Chemother. 67, 2848–2853.
Camarda, A., et al., 2013. Resistance genes, phage types and pulsed field gel electrophoresis pulsotypes in *Salmonella enterica* strains from laying hen farms in southern Italy. Int. J. Environ. Res. Public Health 10, 3347–3362.
Cambray, G., et al., 2010. Integrons. Annu. Rev. Genet. 44, 141–166.
Camps, M., 2010. Modulation of ColE1-like plasmid replication for recombinant gene expression. Recent Pat. DNA Gene Seq. 4, 58–73.
Cannon, P.M., Strike, P., 1992. Complete nucleotide sequence and gene organization of plasmid NTP16. Plasmid. 27, 220–230.
Carattoli, A., et al., 2005. Identification of plasmids by PCR-based replicon typing. J. Microbiol. Methods 63, 219–228.
Chan, P.T., et al., 1985. Nucleotide sequence and gene organization of ColE1 DNA. J. Biol. Chem. 260, 8925–8935.
Curiao, T., et al., 2011. Association of composite IS26-sul3 elements with highly transmissible IncI1 plasmids in extended-spectrum-beta-lactamase-producing Escherichia coli clones from humans. Antimicrob. Agents Chemother. 55, 2451–2457.
De Vito, D., et al., 2015. Diffusion and persistence of multidrug resistant Salmonella typhimurium strains phage type DT120 in southern Italy. Biomed. Res. Int. 2015, 265042.
Domingues, S., et al., 2015. Global dissemination patterns of common gene cassette arrays in class 1 integrons. Microbiology 161, 1313–1337.
Echeita, M.A., et al., 2001. Atypical, fljB-negative Salmonella enterica subsp. enterica strain of serovar 4,5,12:i:- appears to be a monophasic variant of serovar typhimurium. J. Clin. Microbiol. 39, 2981–2983.
Foster, T.J., et al., 1981. Genetic organization of transposon Tn10. Cell 23, 201–213.
Furuya, N., Komano, T., 1997. Mutational analysis of the R64 oriT region: requirement for precise location of the NikA-binding sequence. J. Bacteriol. 179, 7291–7297.
Gruber, A.R., et al., 2008. The Vienna RNA websuite. Nucleic Acids Res. 36, W70–W74.
Guynet, C., de la Cruz, F., 2011. Plasmid segregation without partition. Mob. Genet. Elem. 1, 236–241.
Hall, R.M., Collis, C.M., 1995. Mobile gene cassettes and integrons: capture and spread of genes by site-specific recombination. Mol. Microbiol. 15, 593–600.
Harmer, C.J., Hall, R.M., 2015. IS26-mediated precise excision of the IS26-aphA1a Translocatable unit. MBio 6 (e01866-15).
Harmer, C.J., Hall, R.M., 2016. IS26-mediated formation of transposons carrying antibiotic resistance genes. mSphere 1.
Harmer, C.J., Hall, R.M., 2017. Targeted conservative formation of cointegrates between two DNA molecules containing IS26 occurs via strand exchange at either IS end. Mol. Microbiol. 106, 409–418.
Harmer, C.J., et al., 2014. Movement of IS26-associated antibiotic resistance genes occurs via a translocatable unit that includes a single IS26 and preferentially inserts adjacent to another IS26. MBio 5, e01801–e01814.
He, S., et al., 2015. Insertion sequence IS26 reorganizes plasmids in clinically isolated multidrug-resistant Bacteria by replicative transposition. MBio 6.
Klucar, L., et al., 2010. phiSITE: database of gene regulation in bacteriophages. Nucleic Acids Res. 38, D366–D370.
Lambert, C.M., et al., 1987. Conjugal mobility of the multicopy plasmids NTP1 and NTP16. Plasmid 18, 99–110.
Leipe, D.D., et al., 2002. Classification and evolution of P-loop GTPases and related ATPases. J. Mol. Biol. 317, 41–72.
Liebert, C.A., et al., 1999. Transposon Tn21, flagship of the floating genome. Microbiol. Mol. Biol. Rev. 63, 507–522.
Lorenz, R., et al., 2011. ViennaRNA Package 2.0. Algorithms Mol. Biol. 6, 26.
Lutkenhaus, J., 2012. The ParA/MinD family puts things in their place. Trends Microbiol. 20, 411–418.
Lutkenhaus, J., Sundaramoorthy, M., 2003. MinD and role of the deviant Walker a motif, dimerization and membrane binding in oscillation. Mol. Microbiol. 48, 295–303.
Madeira, F., et al., 2019. The EMBL-EBI search and sequence analysis tools APIs in 2019. Nucleic Acids Res. 47, W636–W641.
Marchler-Bauer, A., et al., 2017. CDD/SPARCLE: functional classification of proteins via subfamily domain architectures. Nucleic Acids Res. 45, D200–D203.
Miriagou, V., et al., 2006. Antimicrobial resistance islands: resistance gene clusters in Salmonella chromosome and plasmids. Microbes Infect. 8, 1923–1930.
Mollet, B., et al., 1985. Gene organization and target specificity of the prokaryotic mobile genetic element IS26. Mol Gen Genet 201, 198–203.
Moran, R.A., Hall, R.M., 2017. Analysis of pCERC7, a small antibiotic resistance plasmid from a commensal ST131 Escherichia coli, defines a diverse group of plasmids that include various segments adjacent to a multimer resolution site and encode the same NikA relaxase accessory protein enabling mobilisation. Plasmid 89, 42–48.
Moran, R.A., Hall, R.M., 2018. Evolution of regions containing antibiotic resistance genes in FII-2-FIB-1 ColV-Colla virulence plasmids. Microb. Drug Resist. 24, 411–421.
Moran, R.A., Hall, R.M., 2019. pBuzz: a cryptic rolling-circle plasmid from a commensal Escherichia coli has two inversely oriented oriTs and is mobilised by a B/O plasmid. Plasmid 101, 10–19.
Moran, R.A., et al., 2016. pCERC3 from a commensal ST95 Escherichia coli: a ColV virulence-multiresistance plasmid carrying a sul3-associated class 1 integron. Plasmid 84-85, 11–19.
Murray, M.G., Thompson, W.F., 1980. Rapid isolation of high molecular weight plant DNA. Nucleic Acids Res. 8, 4321–4325.
Oliva, M., et al., 2017. A novel group of IncQ1 plasmids conferring multidrug resistance. Plasmid 89, 22–26.

Oliva, M., et al., 2018. IS26 mediated antimicrobial resistance gene shuffling from the chromosome to a mosaic conjugative FII plasmid. Plasmid 100, 22–30.
Partridge, S.R., et al., 2009. Gene cassettes and cassette arrays in mobile resistance integrons. FEMS Microbiol. Rev. 33, 757–784.
Partridge, S.R., et al., 2018. Mobile genetic elements associated with antimicrobial resistance. Clin. Microbiol. Rev. 31.
Paul, S., et al., 2016. Corrected genome annotations reveal gene loss and antibiotic resistance as drivers in the fitness evolution of Salmonella enterica Serovar typhimurium. J. Bacteriol. 198, 3152–3161.
Ramsay, J.P., Firth, N., 2017. Diverse mobilization strategies facilitate transfer of non-conjugative mobile genetic elements. Curr. Opin. Microbiol. 38, 1–9.
Ramsay, J.P., et al., 2016. An updated view of plasmid conjugation and mobilization in Staphylococcus. Mobile Genet. Elements 6, e1208317.
Rao, D.N., et al., 2014. Type III restriction-modification enzymes: a historical perspective. Nucleic Acids Res. 42, 45–55.
Reid, C.J., et al., 2015. Tn6026 and Tn6029 are found in complex resistance regions mobilised by diverse plasmids and chromosomal islands in multiple antibiotic resistant Enterobacteriaceae. Plasmid 80, 127–137.
Roberts, R.J., et al., 2015. REBASE–a database for DNA restriction and modification: enzymes, genes and genomes. Nucleic Acids Res. 43, D298–D299.
Rozwandowicz, M., et al., 2018. Plasmids carrying antimicrobial resistance genes in Enterobacteriaceae. J. Antimicrob. Chemother. 73 (5), 1121–1137.
Sampei, G., et al., 2010. Complete genome sequence of the incompatibility group I1 plasmid R64. Plasmid 64, 92–103.
Seemann, T., 2014. Prokka: rapid prokaryotic genome annotation. Bioinformatics 30, 2068–2069.
Shimada, T., et al., 2014. The whole set of constitutive promoters recognized by RNA polymerase RpoD holoenzyme of Escherichia coli. PLoS One 9, e90447.
Smillie, C., et al., 2010. Mobility of plasmids. Microbiol. Mol. Biol. Rev. 74, 434–452.
Stokes, H.W., Gillings, M.R., 2011. Gene flow, mobile genetic elements and the recruitment of antibiotic resistance genes into gram-negative pathogens. FEMS Microbiol. Rev. 35, 790–819.
Suhartono, S., et al., 2018. Transmissible plasmids and Integrons shift Escherichia coli population toward larger multiple drug resistance numbers. Microb. Drug Resist. 24, 244–252.
Tanwar, J., et al., 2014. Multidrug resistance: an emerging crisis. Interdisc.Perspect. Infect. Dis. 2014, 541340.
Tomizawa, J., Itoh, T., 1981. Plasmid ColE1 incompatibility determined by interaction of RNA I with primer transcript. Proc. Natl. Acad. Sci. U. S. A. 78, 6096–6100.
Turlan, C., Chandler, M., 1995. IS1-mediated intramolecular rearrangements: formation of excised transposon circles and replicative deletions. EMBO J. 14, 5410–5421.
Varsaki, A., et al., 2009. Analysis of ColE1 MbeC unveils an extended ribbon-helix-helix family of nicking accessory proteins. J. Bacteriol. 191, 1446–1455.
Varsaki, A., et al., 2012. Interaction between relaxase MbeA and accessory protein MbeC of the conjugally mobilizable plasmid ColE1. FEBS Lett. 586, 675–679.
Zheng, W., et al., 2020. Clinical class 1 integron-integrase gene - a promising indicator to monitor the abundance and elimination of antibiotic resistance genes in an urban wastewater treatment plant. Environ. Int. 135, 105372.